



Syntheses of Isoquinoline and Substituted Quinolines in Charged Microdroplets

Shibdas Banerjee and Richard N. Zare*

Abstract: A Pomeranz–Fritsch synthesis of isoquinoline and Friedländer and Combes syntheses of substituted quinolines were conducted in charged microdroplets produced by an electrospray process at ambient temperature and atmospheric pressure. In the bulk phase, all of these reactions are known to take a long time ranging from several minutes to a few days and to require very high acid concentrations. In sharp contrast, the present report provides clear evidence that all of these reactions occur on the millisecond timescale in the charged microdroplets without the addition of any external acid. Decreasing the droplet size and increasing the charge of the droplet both strongly contribute to reaction rate acceleration, suggesting that the reaction occurs in a confined environment on the charged surface of the droplet.

Isoquinoline and quinoline are isomeric benzopyridines, and appear as structural backbones of many naturally occurring alkaloids.^[1] These benzopyridines have many important applications and are used for synthesizing anesthetics, anti-hypertension agents, antifungal agents, disinfectants, vasodilators, dyes, and pigments, for example, and they are also employed as feedstock in the production of several other specialty chemicals.^[1,2] Most modern methods of synthesizing these heterocycles require high acid/base concentrations and/or high temperatures. Furthermore, in certain cases, the synthesis requires from hours to days to yield significant amounts of product.^[3] In sharp contrast, the present study shows syntheses of isoquinoline and substituted quinolines on the millisecond timescale, using charged microdroplets produced by an electrospray process^[4] at room temperature and atmospheric pressure. With this synthetic procedure, we provide some mechanistic insights into how these reactions occur in the confined charged environment of a droplet.

Electrospray (ES) is a spray-based ambient ionization technique that results in the formation of charged microdroplets (aerosol).^[4,5] Although electrospray ionization (ESI) is extensively used as a soft ionization technique to transfer analytes from solution to the gas phase in mass spectrometry (MS),^[4–6] it also raised our interest for its use to conduct organic synthesis in charged microdroplets. A number of recent studies,^[7] including work of our own,^[8] have reported the acceleration of reaction rates in confined environments. The present study once again demonstrates a remarkable

enhancement in reaction rate, but more importantly, we are able to provide insights explaining the origin of this effect.

An electrospray droplet, which is produced under positive potential, is highly acidic in nature because of the accumulation of protons by solvent oxidation.^[4b,6a] We take advantage of this unique charged environment to induce acid-catalyzed chemical reactions without the addition of any external acid. We investigated the synthesis of isoquinoline and substituted quinolines in charged electrospray droplets by performing three named reactions that are catalyzed by acids, specifically the Pomeranz–Fritsch synthesis of isoquinoline,^[3a] the Friedländer quinoline synthesis,^[9] and the Combes quinoline synthesis.^[10]

Methanolic solutions of reactants were electrosprayed (Figure 1; see also the Supporting Information, Note S1) to produce charged droplets encapsulating the reactants. The

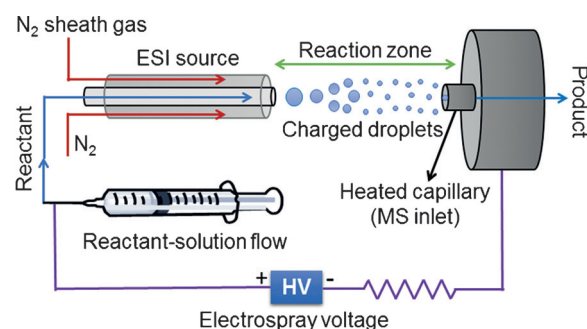


Figure 1. Experimental set-up used to initiate and monitor the synthesis of isoquinoline and substituted quinolines in charged microdroplets.

details of the experimental procedure are presented in the Supporting Information. The Pomeranz–Fritsch reaction^[3,11] is an acid-promoted synthesis of isoquinoline from benzaldehyde and a 2,2-dialkoxyethylamine (Figure 2, top). In the bulk phase, the synthesis is carried out in two steps, namely the condensation of benzaldehyde (**1**) and 2,2-dialkoxyethylamine **2** to form the benzalaminoacetal **3**, followed by acid-induced ring closure via intermediates **4** and **5** to yield isoquinoline **6**.^[3b] The second, acid-catalyzed step requires a high acid concentration (typically ca. 70 % sulfuric acid) as well as a long reaction time, ranging from hours to days.^[3a] We separately prepared intermediate **3** (shown in the cyan circle in Figure 2; see also the chromatographic data in Figures S1 and S2), which was electrosprayed from a methanolic solution as depicted in Figure 1. In sharp contrast to the behavior in bulk solution, in charged microdroplets, we observed the production of isoquinoline from benzalaminoacetal **3**, which

[*] S. Banerjee, Prof. R. N. Zare
Stanford University, Department of Chemistry
333 Campus Drive - Room 133, Stanford, CA 94305-5080 (USA)
E-mail: zare@stanford.edu

Supporting information for this article is available on the WWW under <http://dx.doi.org/10.1002/anie.201507805>.

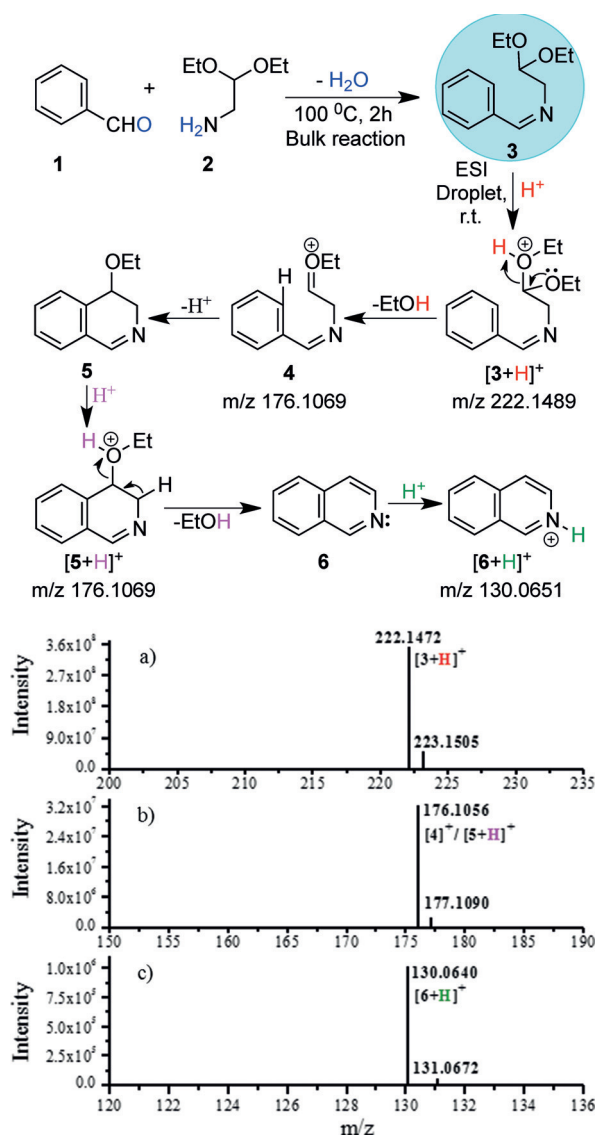


Figure 2. Pomeranz–Fritsch synthesis of isoquinoline in charged microdroplets. Top: two-step synthesis of isoquinoline. First, the conventional bulk reaction method was used to synthesize the precursor imine **3** by reacting **1** and **2**. Second, precursor **3** was electrospayed from a methanolic solution (see Figure 1) to form charged droplets encapsulating the precursor **3** (shown in the cyan circle), which was then converted into isoquinoline **6** via intermediates **4** and **5**. All species, namely precursor **3** (a), intermediates **4** and **5** (b), and product **6** (c) were detected by a high-resolution Orbitrap mass spectrometer. For each of the m/z subsets (a, b, and c), the scales are different. The theoretical m/z values (see scheme) are in good agreement with the experimentally observed ones.

has been registered in the corresponding mass spectrum (Figure 2, bottom), even though the average lifetime of the charged droplet was on the order of milliseconds^[4b,12] and no acid had been added to induce the reaction. Moreover, we detected the intermediates **4** and **5** (not distinguishable by m/z ; see Figure 2), which had been proposed earlier, but not been experimentally observed. To obtain more insights into how these intermediates are formed, we carried out hydrogen–deuterium exchange (HDX) experiments by electro-

spraying a deuterated methanolic (CD_3OD) solution of **3** (Figure S3). We observed that only 12 % of the intermediates (**4** and **5**) had been labelled with deuterium (Figure S3b), and only about 6 % of product **6** were found to be deuterated (Figure S3c). These results indicate that the transformation of **4** into **6** mostly occurs by internal hopping of the protons released by **4** and $[\mathbf{5} + \text{H}]^+$.

The Friedländer synthesis^[9,13] is also an acid-catalyzed process for producing quinolines from *ortho*-aminoaryl aldehydes or ketones and a ketone. In the bulk phase, the synthesis is carried out in the presence of strong acids, such as trifluoroacetic acid (TFA), toluenesulfonic acid (TsOH), and sulfuric acid (H_2SO_4), or in the presence of expensive Lewis acids. The reaction times range from several minutes to several hours depending on the choice of reagents and catalysts.^[13b,14] The reaction is believed to proceed through two parallel routes (Figure 3, top).^[14f]

In the first route, 2-aminoacetophenone (**7**) and carbonyl compound **8** react in a rate-limiting step to form an α,β -unsaturated carbonyl compound **10a** via the aldol adduct **10** followed by water elimination. Compound **10a** then undergoes ring closure, by means of a Schiff base formation

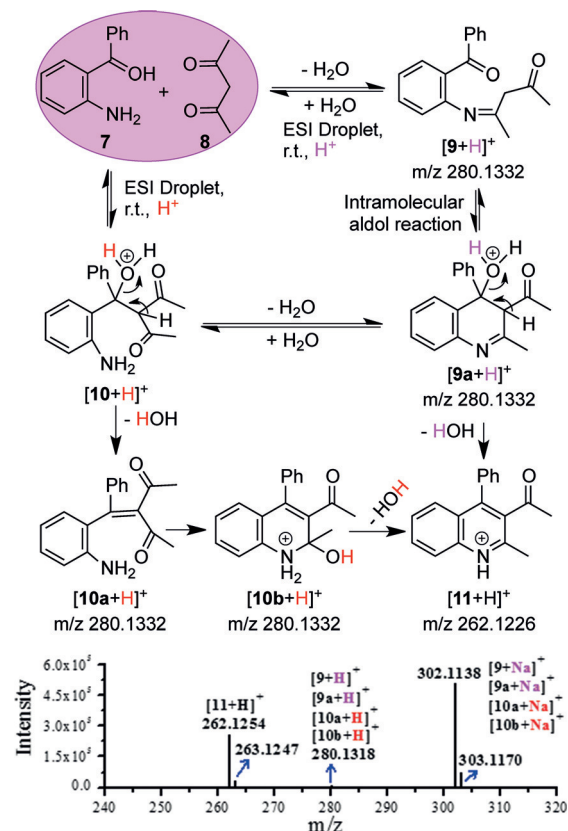


Figure 3. Friedländer synthesis of a substituted quinoline in charged microdroplets. Top: A mixture of reagents **7** and **8** was electrospayed from a methanolic solution (see Figure 1) to form charged droplets encapsulating the reagents **7** and **8** (shown in the pink circle), which were then converted into quinoline **11** via intermediates **9a** and **10a**. All species (intermediates **9**, **9a**, **10a**, and **10b** and product **11**) were detected with a high-resolution Orbitrap mass spectrometer (bottom). The theoretical m/z values (see scheme) are in good agreement with the experimentally observed ones.

reaction, through the intermediate **10b** to yield quinoline **11** by the elimination of another water molecule. In the second route, Schiff base **9** is formed by the condensation reaction of 2-aminobenzophenone (**7**) and carbonyl compound **8** by the elimination of water followed by an intramolecular aldol condensation to yield quinoline **11** after elimination of another water molecule via intermediate **9a**.

Although the thermal condensation of 2-aminobenzophenone (**7**) and acetylacetone (**8**) was not successful, even when conducted at 100 °C for 17 h, we electrosprayed a mixture of **7** and **8** (pink circle in Figure 3) from methanolic solution. In contrast to the reaction in bulk solvent, this bimolecular reaction in ES droplets occurred, again on the millisecond timescale (droplet lifetime),^[4b,12] to form quinoline **11** via several intermediates although no external acid had been added to induce the reaction. The formation of **11** in the ES droplet was confirmed by the corresponding mass spectrum, which showed an intense ion signal at m/z 262.1254 (Figure 3). Although the structures of the intermediates (**9**, **9a**, **10a**, and **10b**; **10** was not detected) could not be distinguished by the present study, an HDX experiment (see Figure S4) indicated the presence of a number of exchangeable protons in the above intermediates, which is in accordance to their structures.

The Combes reaction^[3b,15] is another type of acid-catalyzed synthesis of quinolines (Figure 4, top) by the condensation of aniline **12** and β -diketone **8**. In the bulk phase, the synthesis is carried out in two steps.^[15b] The first step involves the formation of Schiff base **13** by the reaction of aniline **12** and a β -diketone **8**. In the second step, acid is added, and the Schiff base **13** tautomerizes to form enamine **14**, which undergoes in situ annulation followed by water elimination to form the 2,4-substituted quinoline **17** via intermediates **15** and **16**.^[15b] The second step requires a high temperature and a high concentration of strong acids, such as H_2SO_4 , TFA, hydrofluoric acid, or polyphosphoric acid, and the synthesis requires from hours to days.^[3b,16] However, in the present study, we separately prepared intermediate **13** (see the chromatographic data in Figure S5) and electrosprayed it from a methanolic solution. Again, unlike the reaction in bulk solvent, the reaction in ES droplets occurred on the millisecond timescale to form the product quinoline **17** although no acid was added to induce the reaction. The formation of **17** in charged microdroplets was indicated by the ion signal at m/z 158.0964 in the corresponding mass spectrum (Figure 4). Once again, HDX experiments were performed on this reaction. We observed a number of exchangeable protons from intermediates in accordance to their structures (Figure S6).

All of the above studies suggest the feasibility of multistep unimolecular bond rearrangements and elimination reactions catalyzed by the droplet protons. As the ES droplet protons are generated by solvent oxidation, and unlike normal Brønsted acids, they lack their counterions (conjugate bases) in droplets,^[4b,6a] they are anticipated to be powerful acids to promote these reactions and cause the reaction to be much faster than in conventional bulk phase. Furthermore, repeated solvent evaporation and Coulomb fission of the droplet would increase the proton density and thereby

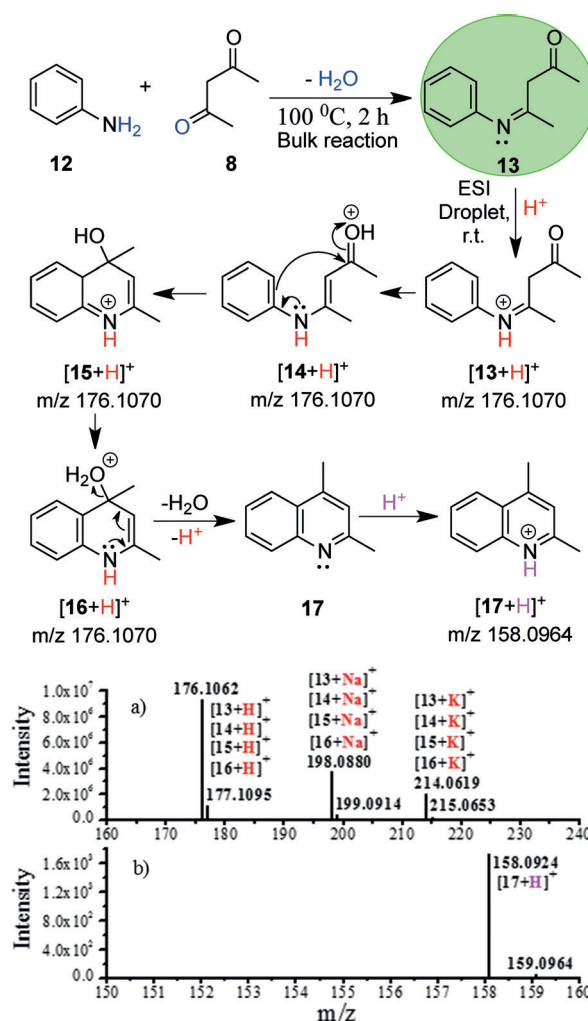


Figure 4. Combes quinoline synthesis in charged microdroplets. Top: two-step synthesis of a substituted quinoline. First, the conventional bulk reaction method was used to synthesize the precursor imine **13** by reacting **12** and **8**. Second, the precursor **13** was electrosprayed from a methanolic solution (see Figure 1) to form charged droplets encapsulating the precursor **13** (shown in the green circle), which was then converted into quinoline **17** inside the charged droplets via intermediates **14**, **15**, and **16**. All protonated species, namely precursor **13** and intermediates **14**, **15**, and **16** (a) and product **17** (b) were detected with a high-resolution Orbitrap mass spectrometer. For each of the m/z subsets (a and b), the scales are different. The theoretical m/z values (see scheme) are in good agreement with the experimentally observed ones.

continuously lower the pH value of the droplet.^[4b,18] Moreover, the protons in the droplet are distributed on its surface with roughly equidistant spacing to minimize the potential energy.^[4b,5a] Therefore, the above reactions (Figures 2–4) are expected to occur on or near to the surface of the droplet; hence, the air–droplet interface should play an important role in accelerating these reactions in this confined environment.

Solvation at the surface is not expected to be the same as solvation in the core of the droplet. Therefore, the possibility of contact ion pairing of the protonated species with the anion (if any) is more prominent in the core than at the surface. Smid has pointed out that loose or solvent-separated ion pairs

may be many times more reactive than contact ion pairs.^[17] This fact may also contribute to enhancing the reaction rate at the droplet surface.

To determine the role of surface protons in influencing the reaction kinetics, we have performed these reactions in ES droplets produced at different flow rates of the reactant solutions (Figure S7) and at different voltages applied to the electrospray source (Figure S8). For each of the three reactions, the reactivity (enhanced efficiency of product formation) increased by more than a factor of five in going from high flow rates (20 $\mu\text{L min}^{-1}$) to low flow rates (0.2 $\mu\text{L min}^{-1}$), which leads to smaller droplets with higher surface-to-volume ratios.^[12,19] Likewise, Figure S8 demonstrates that for each of the three reactions, the reactivity of the reactants increased by more than a factor of five in going from 1 kV to 5 kV applied voltage to the ES source, which leads to more highly charged droplets.^[12] Therefore, the above studies clearly suggest the important role of the ES droplet surface environment on the reaction rate acceleration. The reaction is facilitated by abundant charging of the microdroplets with a high effective surface area.

This reaction rate acceleration can also be attributed to the effects of droplet jet fission (asymmetric Coulomb fission) leading to a stream of tiny offspring droplets, which are known to hold about 2% of the mass and about 15% of the charge of the parent droplet.^[12] The charges are distributed on the surface, and analytes are partitioned in the volume of the droplet, which explains the above unequal distribution. Therefore, smaller offspring droplets are better candidates for promoting these reactions, which is consistent with the reason why these reactions were accelerated by low flow rates (Figure S7).

It should be noted that in Figures 2–4, the comparatively low ion current (intensity) of the product peak compared to that of the reactant peak does not reflect a low reaction yield. Apart from analyte concentration, the ion signal intensity also depends on the ionization efficiency of the analyte.^[20] Structural analyses suggest that the gas-phase basicity of the product is likely to be lower than that of the reactant in all three reactions studied. Therefore, the ion current of the product is expected to be lower compared to that of the reactant when equivalent amounts of reactants and products are present. Comparing the conventional bulk-phase reaction yield (%) in a given time,^[3,13,14f,15] we calculated the reaction rate acceleration in charged microdroplets (see Note S2), which was found to be more than a factor of 10^6 for the Pomeranz–Fritsch synthesis (Figure 2), more than a factor of 10^5 for the Friedländer synthesis (Figure 3), and more than a factor of 10^3 for the Combes synthesis (Figure 4), assuming that the ionization efficiencies of product and reactant are the same (Figures 2–4). The above calculation is only a rough estimate, and more detailed quantitative analyses of the above reactions need to be undertaken.

HPLC-ESI-MS analyses show unequivocally that the precursors of the Pomeranz–Fritsch reaction (Figure S2) and the Combes reaction (Figure S5) were transformed into the products in the ES droplets rather than in the bulk phase prior to nebulization. Aside from reaction rate acceleration, this method of synthesis in microdroplets would also have

potential applications to identify intermediate(s) of the reaction by using mass spectrometric or spectroscopic techniques that analyze the chemical content of the microdroplets.^[7d,8]

In summary, we have synthesized isoquinoline by the Pomeranz–Fritsch reaction starting with intermediate **3** and substituted quinolines by the Friedländer synthesis starting with **7** and **8** as well as by the Combes synthesis starting with intermediate **13**. All of these reactions were carried out in charged microdroplets under ambient conditions. The reactions were shown to be catalyzed by the surface protons of the ES droplets although no external acids were added to the aspirating solution to induce the reaction. Therefore, the present method circumvents the need for expensive acid catalysts, high temperatures, and long reaction times that are associated with the above syntheses when carried out in traditional ways. Thus charged microdroplets can be viewed as “tiny reaction vessels” for these reactions.

Furthermore, the reactions occurred on the millisecond timescale in the charged microdroplets, suggesting a remarkable acceleration of reaction rates. Moreover, the reaction efficiency was improved in smaller droplets (higher surface-to-volume ratio) and in droplets with abundant surface charges (protons). Previous work has shown that charges (H^+) in the electrosprayed microdroplet reside primarily on the surface to minimize the potential energy.^[4b,5a] Moreover, as the microdroplet size decreases, the importance of the surface grows. Thus we believe that the enhancement of the reaction rate comes from the proton-catalyzed surface reaction. We conclude that reactions in the confined environment can occur in a different manner to those in a bulk environment. This “microdroplet chemistry” is still in its infancy and heightens our interests to apply this method to organic syntheses on the preparative scale.^[7c]

Acknowledgements

This work was supported by the Air Force Office of Scientific Research through a Basic Research Initiative grant (AFOSR, FA9550-12-1-0400) and the National Science Foundation under the CCI Center for Selective C–H Functionalization (CHE-1205646).

Keywords: acid catalysis · electrospray · mass spectrometry · protonation · reaction mechanisms

How to cite: *Angew. Chem. Int. Ed.* **2015**, *54*, 14795–14799
Angew. Chem. **2015**, *127*, 15008–15012

- [1] a) E. Fattorusso, O. Tagliatela-Scafati, *Modern Alkaloids: Structure, Isolation, Synthesis and Biology*, Wiley, Weinheim, **2008**; b) K. C. Majumdar, S. K. Chattopadhyay, *Heterocycles in Natural Product Synthesis*, Wiley, Weinheim, **2011**.
- [2] a) J. J. Li, *Heterocyclic Chemistry in Drug Discovery*, Wiley, New York, **2013**; b) H. G. Franck, J. W. Stadelhofer, *Industrial Aromatic Chemistry: Raw Materials · Processes · Products*, Springer, Berlin/Heidelberg, **2012**; c) G. Collin, H. Höke in *Ullmann's Encyclopedia of Industrial Chemistry*, Wiley-VCH, Weinheim, **2000**.

- [3] a) W. J. Gensler in *Organic Reactions*, Wiley, New York, **2004**; b) J. J. Li, *Name Reactions: A Collection of Detailed Mechanisms and Synthetic Applications, Fifth Edition*, Springer, Switzerland, **2014**; c) E. Schlittler, J. Müller, *Helv. Chim. Acta* **1948**, *31*, 914–924.
- [4] a) J. Fenn, M. Mann, C. Meng, S. Wong, C. Whitehouse, *Science* **1989**, *246*, 64–71; b) S. Banerjee, S. Mazumdar, *Int. J. Anal. Chem.* **2012**, 282574.
- [5] a) J. B. Fenn, *J. Am. Soc. Mass Spectrom.* **1993**, *4*, 524–535; b) S. Banerjee, S. Mazumdar, *J. Am. Soc. Mass Spectrom.* **2012**, *23*, 1967–1980.
- [6] a) G. J. Van Berkel, V. Kertesz in *Electrospray and MALDI Mass Spectrometry*, Wiley, Hoboken, **2010**, pp. 75–122; b) S. Banerjee, S. Mazumdar, *J. Mass Spectrom.* **2010**, *45*, 1212–1219.
- [7] a) S. Banerjee, *J. Mass Spectrom.* **2013**, *48*, 193–204; b) S. Banerjee, H. Prakash, S. Mazumdar, *J. Am. Soc. Mass Spectrom.* **2011**, *22*, 1707–1717; c) R. M. Bain, C. J. Pulliam, R. G. Cooks, *Chem. Sci.* **2015**, *6*, 397–401; d) T. Müller, A. Badu-Tawiah, R. G. Cooks, *Angew. Chem. Int. Ed.* **2012**, *51*, 11832–11835; *Angew. Chem.* **2012**, *124*, 12002–12005; e) A. Fallah-Araghi, K. Meguellati, J.-C. Baret, A. E. Harrak, T. Mangeat, M. Karplus, S. Ladame, C. M. Marques, A. D. Griffiths, *Phys. Rev. Lett.* **2014**, *112*, 028301; f) M. Girod, E. Moyano, D. I. Campbell, R. G. Cooks, *Chem. Sci.* **2011**, *2*, 501–510; g) A. Badu-Tawiah, D. Campbell, R. G. Cooks, *J. Am. Soc. Mass Spectrom.* **2012**, *23*, 1461–1468.
- [8] a) R. H. Perry, M. Splendore, A. Chien, N. K. Davis, R. N. Zare, *Angew. Chem. Int. Ed.* **2011**, *50*, 250–254; *Angew. Chem.* **2011**, *123*, 264–268; b) J. K. Lee, S. Kim, H. G. Nam, R. N. Zare, *Proc. Natl. Acad. Sci. USA* **2015**, *112*, 3898–3903; c) J. K. Lee, S. Banerjee, H. G. Nam, R. N. Zare, *Quart. Rev. Biophys. Discovery* **2015**, DOI: 10.1017/S0033583515000086.
- [9] C.-C. Cheng, S.-J. Yan in *Organic Reactions*, Wiley, New York, **2004**.
- [10] J. J. Li in *Name Reactions*, Springer, Berlin/Heidelberg, **2006**, pp. 144–146.
- [11] a) J. M. Bobbitt, A. J. Bourque, *Heterocycles* **1987**, *25*, 601–616; b) C. Pomeranz, *Monatsh. Chem.* **1893**, *14*, 116–119.
- [12] P. Kebarle, L. Tang, *Anal. Chem.* **1993**, *65*, 972A–986A.
- [13] a) P. Friedlaender, *Ber. Dtsch. Chem. Ges.* **1882**, *15*, 2572–2575; b) A. Shaabani, E. Soleimani, Z. Badri, *Synth. Commun.* **2007**, *37*, 629–635.
- [14] a) C.-S. Jia, Z. Zhang, S.-J. Tu, G.-W. Wang, *Org. Biomol. Chem.* **2006**, *4*, 104–110; b) J. S. Yadav, B. V. S. Reddy, P. Sreedhar, R. S. Rao, K. Nagaiah, *Synthesis* **2004**, 2381–2385; c) R. Varala, R. Enugala, S. R. Adapa, *Synthesis* **2006**, 3825–3830; d) A.-H. Li, D. J. Beard, H. Coate, A. Honda, M. Kadalbajoo, A. Kleinberg, R. Laufer, K. M. Mulvihill, A. Nigro, P. Rastogi, D. Sherman, K. W. Siu, A. G. Steinig, T. Wang, D. Werner, A. P. Crew, M. J. Mulvihill, *Synthesis* **2010**, 1678–1686; e) A. Bañón-Caballero, G. Guillena, C. Nájera, *J. Org. Chem.* **2013**, *78*, 5349–5356; f) J. Marco-Contelles, E. Pérez-Mayoral, A. Samadi, M. d. C. Carreiras, E. Soriano, *Chem. Rev.* **2009**, *109*, 2652–2671.
- [15] a) J. L. Born, *J. Org. Chem.* **1972**, *37*, 3952–3953; b) S. A. Yamashkin, L. G. Yudin, A. N. Kost, *Chem. Heterocycl. Compd.* **1992**, *28*, 845–855.
- [16] a) J. C. Sloop, *J. Phys. Org. Chem.* **2009**, *22*, 110–117; b) P. Evans et al., *Tetrahedron* **2005**, *61*, 9696–9704.
- [17] a) J. Smid, *Angew. Chem. Int. Ed. Engl.* **1972**, *11*, 112–127; *Angew. Chem.* **1972**, *84*, 127–144; b) J. Smid, *J. Polym. Sci. Part A* **2004**, *42*, 3655–3667.
- [18] C. L. Gatlin, F. Turecek, *Anal. Chem.* **1994**, *66*, 712–718.
- [19] K. Tang, A. Gomez, *J. Aerosol Sci.* **1994**, *25*, 1237–1249.
- [20] a) M. Oss, A. Krueve, K. Herodes, I. Leito, *Anal. Chem.* **2010**, *82*, 2865–2872; b) I. Leito, K. Herodes, M. Huopolaenen, K. Virro, A. Künnapas, A. Krueve, R. Tanner, *Rapid Commun. Mass Spectrom.* **2008**, *22*, 379–384.

Received: August 20, 2015

Revised: September 5, 2015

Published online: October 9, 2015